Signal Processing 107 (2015) 302–311

Contents lists available at ScienceDirect

Signal Processing

journal homepage: www.elsevier.com/locate/sigpro

Chaos in fractional and integer order NSG systems ☆

S. Hassan HosseinNia [a,*], Richard L. Magin [b], Blas M. Vinagre [a]

[a] *Industrial Engineering School, University of Extremadura, 06006 Badajoz, Spain*
[b] *Department of Bioengineering, University of Illinois, 851 South Morgan Street, Chicago, IL 60607, USA*

ARTICLE INFO

Article history:
Received 27 December 2013
Received in revised form
24 June 2014
Accepted 25 June 2014
Available online 3 July 2014

Keywords:
Reset control
Fractional control
Clegg integrator
Quadratic stability
Hybrid systems
Servomotor
Magnetic resonance

ABSTRACT

The nuclear spin generator (NSG) is a high-frequency oscillator that generates and controls the oscillations of the precessional motion of a nuclear magnetization vector in a magnetic field. This nonlinear system was first described by S. Sherman in 1963, and exhibits a wide variety of chaotic behavior, but it is not as well studied as the classic Lorenz chaotic system. In this paper, chaos in the integer order nuclear spin generator system is reviewed. In addition, using fractional order stability analysis, the chaotic behavior of the fractional order NSG (FNSG) is studied. The numerical results are obtained using the Adams–Bashforth–Moulton algorithm encoded in the *fde12* Matlab function. In order to confirm the numerically demonstrated chaotic behavior in the nuclear spin generator, we prepared a bifurcation diagram. The phase portrait of the FNSG is also depicted for different fractional orders to show the overall chaotic behavior of the system. These results are also verified using bifurcation analysis. Our results demonstrate a modulating effect on chaos as the fractional order decreases, which could be used to improve the design of the controller in the NSG model. This work also demonstrates how the fractional order model extends the dynamic behavior of the NSG system.

1. Introduction

Fractional order models provide a heuristic approach to the description of complex circuits and systems. In the 'fractional' approach, instead of adding complexity by extending the structure, composition or number of components, we generalize the order of the integer derivatives used to describe the key dynamic processes (e.g., battery charging rate, viscoelastic creep, or electric/magnetic dipole polarization). As with all models, success is characterized by the fidelity with which the predictions fit the observed phenomena, and as articulated by the Polish mathematician, M. Kac, "by the sharpness of the questions they pose about the underlying physics" [1]. Fractional order models are sometimes criticized for what they are not – conceptual models of fundamental laws or theories. In such cases, it is important to identify when using them the specific properties of a complex system that suggest fractional order generalization. Just as Brownian motion is a stochastic model based on the assumptions that the component particles are identical, independent, and have distributions with fixed time and space increments, fractional order models appear to be the most useful for systems that relax these assumptions, and hence, exhibit some degrees of memory or nonlocal behavior.

Nuclear magnetic resonance (NMR), which provides the basis for magnetic resonance imaging (MRI), is fundamentally described by the Bloch equations: a set of linear, first-order ordinary differential equations [2]. This description is adequate for the characterization of simple liquids and for samples with a relatively homogeneous composition [3]. As such, the governing Bloch equations provide the basis for

☆ This study was supported in part by NIH/NIBIB Grant EB007537 awarded to Richard L. Magin and by the Government of Extremadura Grant GR10157 awarded to S. Hassan HosseinNia and Blas M. Vinagre.

* Corresponding author.
E-mail addresses: hoseinia@unex.es (S. Hassan HosseinNia), rmagin@uic.edu (R.L. Magin), bvinagre@unex.es (B.M. Vinagre).

http://dx.doi.org/10.1016/j.sigpro.2014.06.021
0165-1684/

the imaging algorithms of MRI, which can be applied to complex heterogeneous materials such as imaging the human brain [4]. However, in order to optimize the techniques of NMR spectroscopy or to enhance contrast in MRI, it is necessary to append the basic theory with nonlinear, nonlocal and time-dependent processes. Therefore, it is natural to investigate ways in which generalization of the Bloch equations to fractional order can assist in characterizing relaxation, diffusion, and radiation damping in complex tissues and materials.

Early NMR studies by Sherman [5] designed to describe and control the spin dynamics of radiation damping led to a nonlinear extension of the Bloch equations. These modified equations were subsequently shown by Sachdev and Sarathy [6], Abergel [7], Park [8], Yuan and Yang [9], Ahn [10], and Hamri and Houmor [11] to exhibit periodic and chaotic solutions. Such chaos (spin turbulence) was experimentally observed by Jeener [12], Huang et al [13], and by Abergel and Louis-Joseph [14]. Interest in applying feedback control in NMR [15,16], in general, and to prevent chaos, in particular, [17–19] has grown over the past 20 years. Finally, more recently, several groups of investigators [20–22] have begun to examine solutions to the fractional order Bloch equations.

In this paper, we examine – for the first time – chaos in the fractional order Sherman model (nuclear spin generator, NSG) of the Bloch equations. Following an analytical study of inherent system stability, we numerically confirm the onset of chaos through the use of a bifurcation diagram. Our results demonstrate a modulating effect on chaos as the fractional order decreases, which could be used to improve the design of the controller in the NSG model. This work also demonstrates how the fractional order model extends the dynamic behavior of the NSG system.

2. Chaos in the NSG system

2.1. Preliminary

2.1.1. Numerical method

The basic definitions and properties of the fractional calculus used in this paper can be found in [23]. Briefly, we employ the Caputo fractional derivative as a function of time and assume commensurate order generalizations up to order one. The numerical methods used for solving ordinary differential equations (ODEs) need to be modified for solving fractional differential equations (FDEs). A modification of Adams–Bashforth–Moulton algorithm proposed by Diethelm et al. [24–26] to solve FDEs is used in this paper by applying the Matlab code *fde12* developed by Garrappa [27]. This algorithm has been used by many researchers who study chaos in fractional order systems, and has been shown to be robust and reliable [28,29]. All the numerical simulations presented in this paper were performed using the initial conditions $(x(0), y(0), z(0)) = (0.2, 0.05, 0.2)$, and a fixed time step size of $h = 0.001$s.

2.1.2. Stability and chaotic attractors

In a three-dimensional (3-D) nonlinear system, a saddle point is an equilibrium point on which the equivalent linearized model has at least one eigenvalue in the stable region and one in the unstable region. In the same system, a saddle point is called saddle point of index 1 if one of the eigenvalues is unstable and the others are stable. A saddle point of index 2 is a saddle point with one stable eigenvalue and two unstable ones. In chaotic systems,

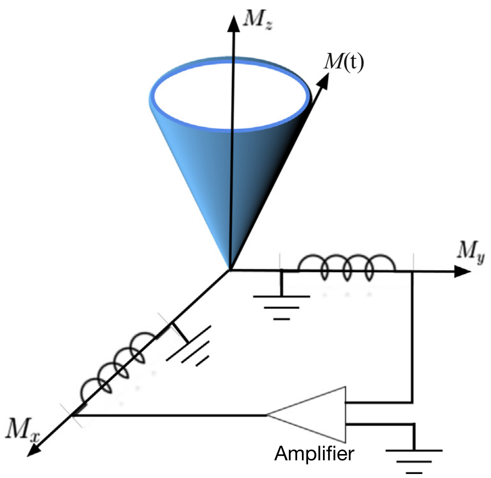

Fig. 1. Nuclear spin generator.

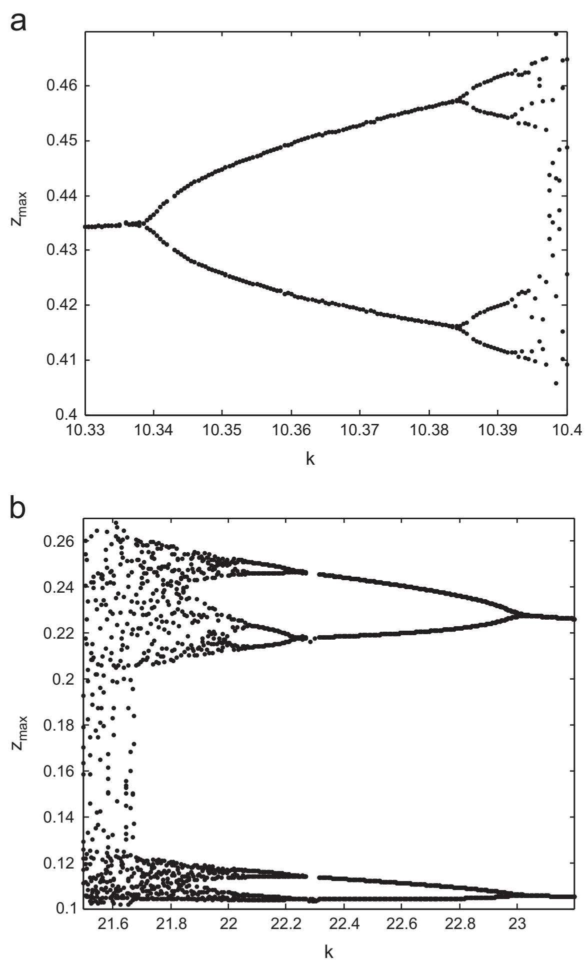

Fig. 2. Bifurcation diagram: (a) $10.33 \le k \le 10.4$ and (b) $21.5 \le k \le 23$.

it is found that scrolls are generated only around saddle points of index 2. The saddle points of index 1 are responsible only for connecting the scrolls. In 3-D commensurate fractional order systems, like their ordinary counterparts, the saddle points of index 2 play a key role in the generation of scrolls [29] (for more details

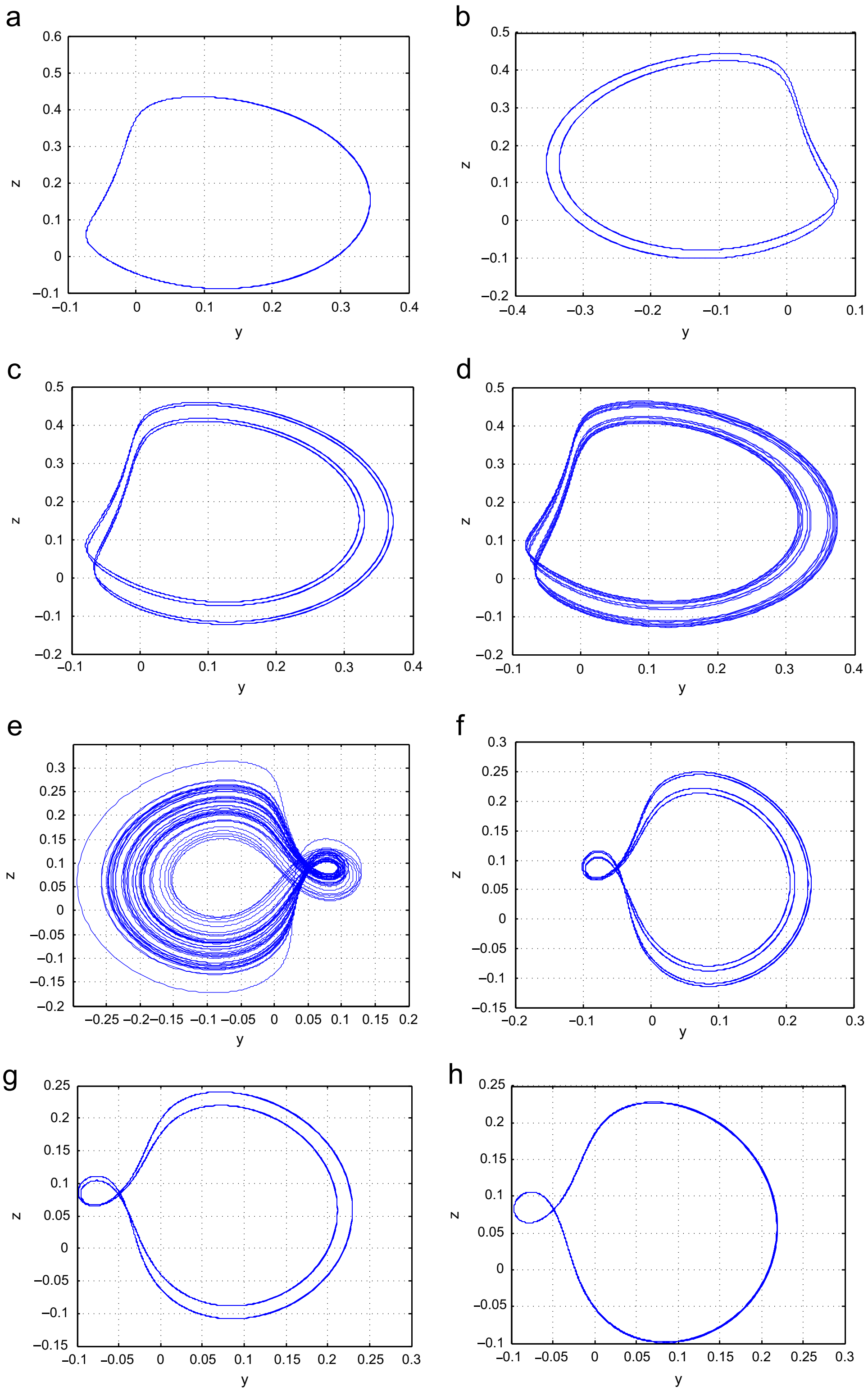

Fig. 3. Phase portrait: (a) $k=10.33$, (b) $k=10.35$, (c) $k=10.39$, (d) $k=10.4$, (e) $k=21.50$, (f) $k=22.10$, (g) $k=22.60$, and (h) $k=23$.

see [30–33]). Consider the case of a fractional commensurate order system of the form [34]:

$$D^q x = f(x) \tag{1}$$

where $0<q<1$ and $x\in\mathbb{R}^n$, the equilibrium points of system (1) are locally asymptotically stable if all eigenvalues (λ) of Jacobian matrix $J=\partial f/\partial x$ at the equilibrium points satisfy

$$|\arg(\lambda)| > q\pi/2. \tag{2}$$

2.2. Chaos in NSG system

As shown in Fig. 1 the NSG system describes the precession of magnetization (M_x, M_y, M_z) in a simple nuclear magnetic resonance (NMR) experiment. An NMR active nuclei (typically a liquid containing H^1, C^{13} or P^{31} nuclei) is positioned at the center of a strong static magnetic field B_0 and surrounded by one or more radio-frequency (RF) coils. The direction of B_0, defines the z-direction in the laboratory reference frame. An exciting RF coil is oriented with its axis in the x-direction, while a pick-up RF coil is oriented with its axis in the y-direction. A high-gain amplifier detects the voltage induced in the pick-up coil and feeds it back to the exciting coil. The time-dependent behavior of the components of the nuclear magnetization vector in this case is given by the Bloch equations with feedback, and the normalized form of the nuclear spin system can be represented by [5,6]

$$\begin{cases} \dot{x} = -\beta x + y \\ \dot{y} = -x-\beta y(1-kz) \\ \dot{z} = \beta(\alpha(1-z)-ky^2) \end{cases} \tag{3}$$

where $(x,y,z)=(M_x,M_y,M_z)$ are the components of the nuclear magnetization vector in the x-, y-, and z-directions, respectively, $\beta=1/T_2$, $\alpha=T_2/T_1$, where T_1 and T_2 are the characteristic spin–lattice and spin–spin NMR relaxation times, respectively. The parameters $\alpha,\beta\geq 0$ are linear damping terms, while the nonlinearity parameter βk is proportional to the amplifier gain in the voltage feedback. Physical considerations limit the parameter α to the range $0<\alpha\leq 1$, while $0.25<\beta<100$ [5].

Sachdev and Sarathy studied this system by finding the values of k leading to chaotic behavior for a given (α,β) couple. They demonstrated that in the case of $\alpha\leq 1$ and $\beta<1$, as k increases from $(1+\beta^2)/\beta^2$, the system goes from period-doubling bifurcation to chaos [6].

Fig. 2 shows the bifurcation diagram of the NSG system for $\alpha=0.15$ and $\beta=0.75$. As can be seen in Fig. 2(a) the periodic behavior occurs when $k<10.34$, and when $10.34<k<10.385$ and $10.385<k<10.393$ the system shows period-doubling and period-quadrupling behavior respectively. The system exhibits chaos at $k\sim 10.393$, and this chaotic behavior persists until $k\sim 22.08$. Above this value of k, there is a qualitative change. As k increases further, the evolution of the trajectories from one half-plane to the other slows down, and the single strange attractor bifurcates into two symmetric strange attractors; the trajectories move into one or the other, depending on their initial conditions (see Fig. 3). As illustrated in Fig. 2(b) the system shows period-quadrupling when k increases from 22.08 to 22.22. Finally, the system will show the period-doubling and periodic behavior for the intervals $22.3<k<23$ and $k>23$, respectively. Fig. 3 shows the phase portrait of the system in the y–z plane for different values of k that are in agreement with the bifurcation diagram. Fig. 3(a) and (h), for example, shows the periodic behavior for $k=10.33$ and $k=23$, respectively. The phase portrait of system for $k=10.35$ and $k=22.6$ shows period-doubling in Fig. 3(b) and (g), and for $k=10.39$ and $k=22.1$ it shows period-quadrupling in Fig. 3(c) and (f), respectively. Finally, chaotic behavior can be seen in Fig. 3(d) and (e) for $k=10.4$ and $k=21.5$, respectively.

3. Chaos in the fractional order NSG system

By replacing the first-order integer derivative by a Caputo fractional derivative of order q (D^q) in (3), we obtain a fractional commensurate order version of the NSG

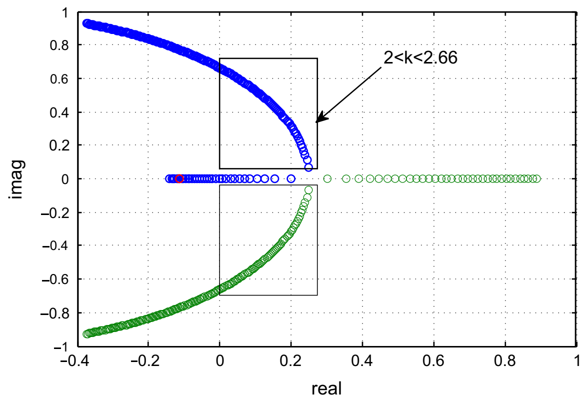

Fig. 4. Root locus of the linearized system through first equilibrium point. (For interpretation of the references to color in this figure caption, the reader is referred to the web version of this paper.)

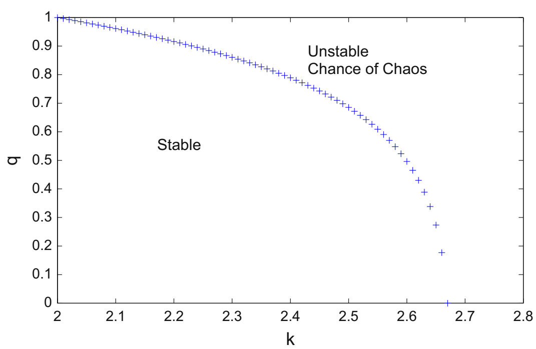

Fig. 5. Stability region for the linearized system through its first equilibrium point $(0,0,1)$.

system (FNSG) as

$$\begin{cases} D^q x = -\beta x + y \\ D^q y = -x - \beta y(1-kz) \\ D^q z = \beta(\alpha(1-z) - ky^2) \end{cases} \tag{4}$$

The aim of the paper is to study the chaotic behavior of this FNSG system. Linearization will be used at the following three equilibrium points:

1. $(x_1, y_1, z_1) = (0, 0, 1)$
2. $(x_2, y_2, z_2) = \left(c, \beta c, \frac{1+\beta^2}{k\beta^2}\right)$
3. $(x_3, y_3, z_3) = \left(-c, -\beta c, \frac{1+\beta^2}{k\beta^2}\right)$

where $c = \sqrt{\alpha(\beta^2(k-1)-1)/k\beta^2}$ and $k > (1+\beta^2)/\beta^2$. The Jacobian matrix of the system evaluated at the equilibrium points $(x_i, y_i, z_i), i = 1, 2, 3$ is

$$\begin{bmatrix} -\beta & 1 & 0 \\ -1 & -\beta(1-kz_i) & k\beta y_i \\ 0 & -2k\beta y_i & -\beta\alpha \end{bmatrix}. \tag{5}$$

Using this information, we can analyze the stability of the system and determine its chaotic behavior for each equilibrium point: the system (4) will be stable if and only if the eigenvalues of the Jacobian matrix satisfy (2), that is, $\lambda_1 = -\beta\alpha$, and $2\lambda_{2,3} = \beta(k-2) \pm \sqrt{k^2\beta^2 - 4}$ for $(x_1, y_1, z_1) = (0, 0, 1)$. As noted in Section 2.1, the system will show chaotic behavior if $\lambda_{2,3}$ are complex conjugates with a positive real part when $2 < k < 2/\beta, \forall 0 < \beta < 1$; therefore, the integer

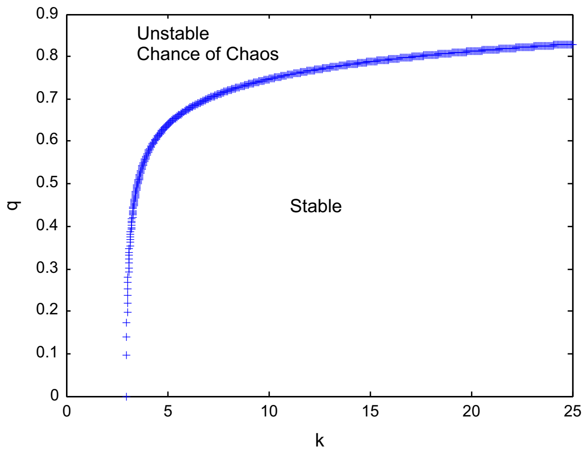

Fig. 7. Stability region for linearized system through second and third equilibrium points.

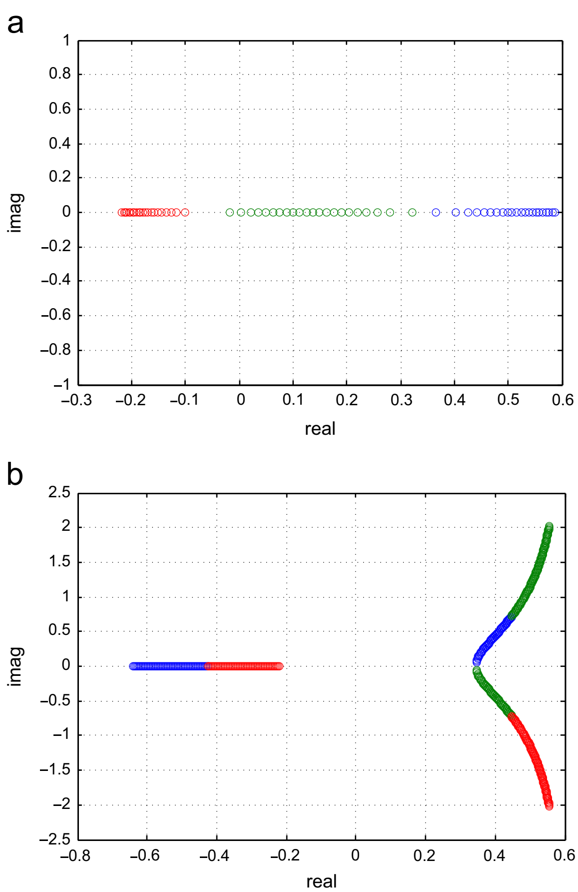

Fig. 6. Root locus of the linearized system through its second and third equilibrium points: (a) $2.78 \le k < 2.99$ and (b) $k \ge 2.99$.

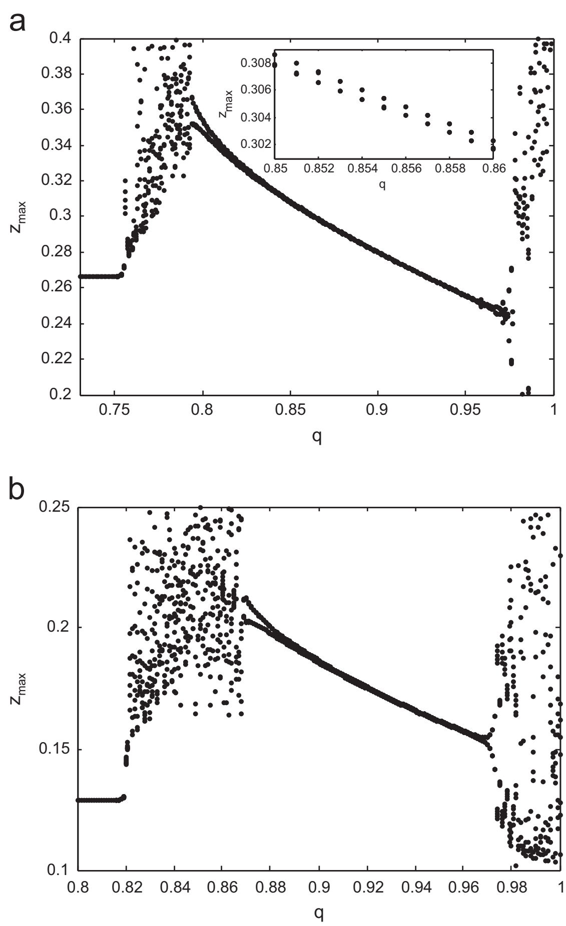

Fig. 8. Bifurcation diagram: (a) $k = 10.5$ and (b) $k = 21.5$.

order system can be chaotic. The root locus of the system for the values of $\alpha = 0.15$ and $\beta = 0.75$ is shown in Fig. 4. In this figure each color shows each λ for all $k > 0$. For fractional order, the system can be chaotic if $|\arg(\lambda_{2,3})| < q\pi/2$. In order to show the probable chaotic region of the system the stability region of the linearized version is shown in Fig. 5 by plotting q versus k.

Now, let us consider the second and third equilibrium points. The corresponding linearized systems are

$$\begin{cases} D^q x = -\beta x + y \\ D^q y = -x + \dfrac{1}{\beta} y + \beta^2 kcz \\ D^q z = -\beta\alpha z - 2\beta^2 kcy \end{cases} \tag{6}$$

and

$$\begin{cases} D^q x = -\beta x + y \\ D^q y = -x + \dfrac{1}{\beta} y - \beta^2 kcz \\ D^q z = -\beta\alpha z + 2\beta^2 kcy \end{cases} \tag{7}$$

respectively. The Jacobian matrix of (6) and (7) is respectively given by

$$\begin{bmatrix} -\beta & 1 & 0 \\ -1 & \frac{1}{\beta} & k\beta^2 c \\ 0 & -2k\beta^2 c & -\beta\alpha \end{bmatrix}, \tag{8}$$

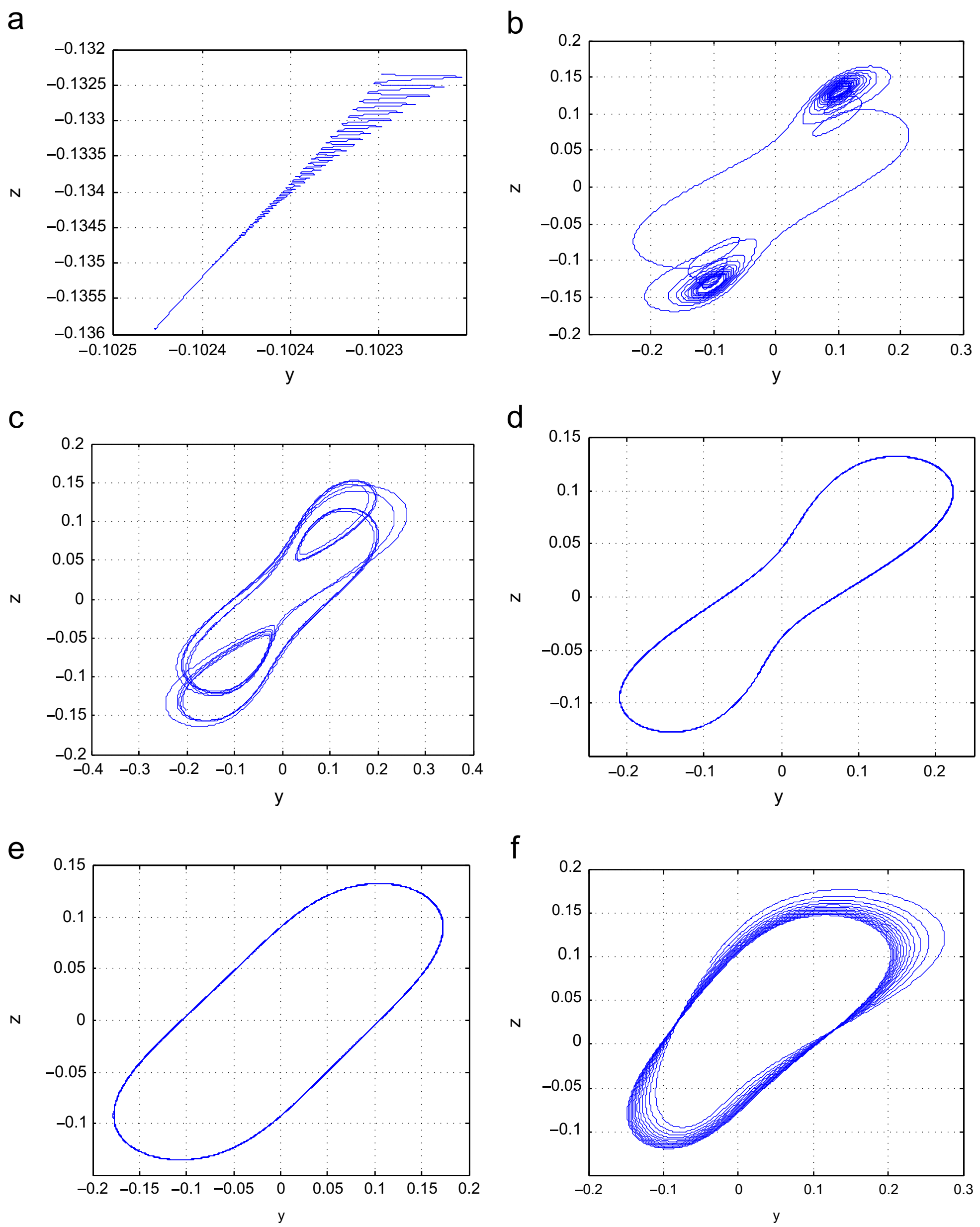

Fig. 9. Phase portrait: (a) $q=0.75$, (b) $q=0.76$, (c) $q=0.794$, (d) $q=0.795$, (e) $q=0.978$, and (f) $q=0.979$.

and

$$\begin{bmatrix} -\beta & 1 & 0 \\ -1 & \frac{1}{\beta} & -k\beta^2 c \\ 0 & 2k\beta^2 c & -\beta\alpha \end{bmatrix}, \tag{9}$$

and the characteristic polynomials corresponding to both systems are

$$\lambda^3+\left(\beta+\alpha\beta-\frac{1}{\beta}\right)\lambda^2+\left(2\alpha\beta^2 k-\alpha\beta^2-3\alpha\right)\lambda \quad +2\alpha\beta^3(k-1)-2\alpha\beta. \tag{10}$$

Therefore, both linearized systems through the equilibrium points (b) and (c) have the same characteristic polynomials, hence the same eigenvalues. As mentioned before, the equilibrium points (a) and (b) are valid for $k>(1+\beta^2)/\beta^2$. Therefore, the root locus of the system is depicted in Fig. 6 for the values of $\alpha=0.15$ and $\beta=0.75$, $k\geq 2.78$. As can be seen, the two eigenvalues of the system are complex conjugates with a positive real part when $k\geq 2.99$, so that the system may show chaotic behavior in this range. Fig. 7 shows the probable chaotic region of the fractional order system plotted versus k.

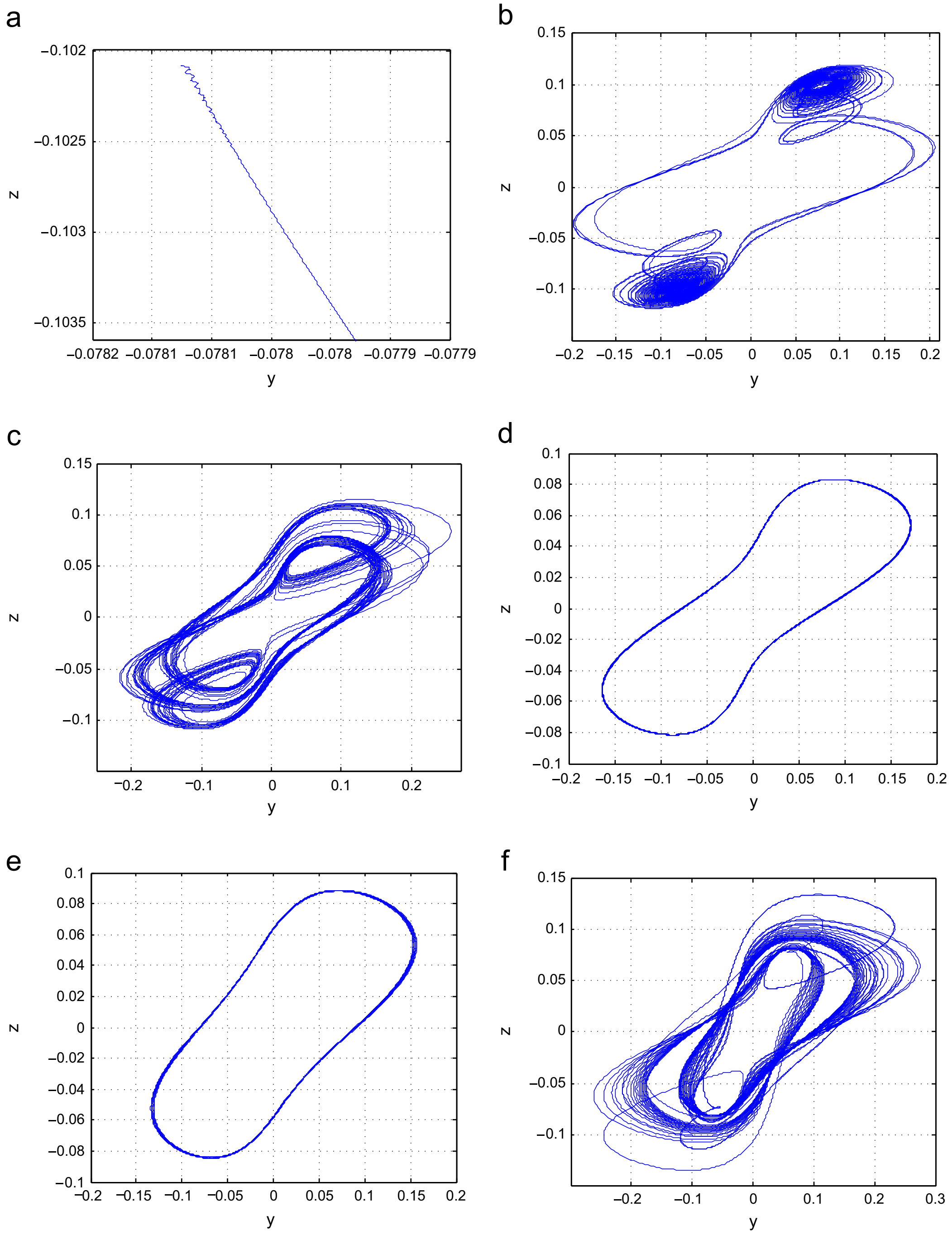

Fig. 10. Phase portrait: (a) $q=0.81$, (b) $q=0.82$, (c) $q=0.867$, (d) $q=0.868$, (e) $q=0.975$, and (f) $q=0.977$.

Now, the chaotic behavior of the fractional order system will be analyzed. For this purpose, the bifurcation diagram of the FNSG system is depicted in Fig. 8. From Fig. 2 we know that the system has chaotic behavior for the interval from $k=10.5$ to $k=21.5$. Therefore, the chaotic behavior of the system is shown using the bifurcation diagram of the system for two different cases i.e., $k=10.5$ and $k=21.5$, in Fig. 8(a) and (b), respectively. From both the figures we can see that as we decrease the fractional order of the derivative, the system goes from chaotic behavior to period-doubling and again goes to chaotic behavior until it achieves the stable region. From Fig. 8(a) the system shows chaotic behavior for $0.751<q<0.795$ and $0.978<q<1$ and shows period-doubling for $0.795 \le q \le 0.978$. Also from Fig. 8(b) the system shows chaotic behavior for $0.818<q<0.868$ and $0.975<q<1$, and shows period-doubling for $0.868 \le q \le 0.975$.

To verify the bifurcation diagram results, phase portraits of the system are shown in Figs. 9 and 10 for $k=10.5$, and $k=21.5$, respectively. Figs. 9(a) and 10(a) show the system to be stable for $q=0.75$, $k=10.5$, and $q=0.81, k=21.5$, respectively. Figs. 9(b), (c), and (f) and 10(b), (c), and (f) show the chaotic behavior of the system for $q=0.76$, $q=0.794$, $q=0.979$, $k=10.5$, and for $q=0.82$, $q=0.867$, $q=0.977$, $k=21.5$. Finally, the system shows period-doubling for $q=0.795$, $q=0.978$, $k=10.5$ and $q=0.868$, $q=0.975$, $k=21.5$ which is shown in Figs. 9(d) and (e) and 10(d) and (e). The results verify the bifurcation and stability analysis.

Fig. 11 shows the stability region of the fractional order system versus parameters α and β. As can be seen in the figure, reduction of the fractional order parameter q leads to a greater likelihood of chaos in the system. It is clear that the system is unstable for almost all values of the fractional order parameter, and for all β less than 0.35. There is a high chance of chaos for a wide range of the fractional order parameter q when $0<\beta<0.8$. On the other hand, for a high value of β, chaos only appears with integer order or when the fractional order is close to one. It also has to be mentioned that except for a very small range of α i.e., $\alpha<0.2$, the stability region is almost unchanged for the entire set of β and q values examined. Therefore, the parameters β, i.e., $1/T_2$ and q have the most significant effects on the stability of the fractional order NSG system.

4. Discussion

The NSG model is an example of a simple – laboratory based – system that exhibits a spectrum of chaotic behavior (e.g., period doubling, intermittency, and the gluing of strange attractors) [6]. Since the behavior of the NSG system is relatively unknown, here we compare the onset of chaos for the FNSG system in the context of the fractional order generalization of a few classic chaotic systems [35,36]. In addition, we connect the FNSG system with the fractional order model of radiation damping (RD) [37] studied by Bhalekar and coworkers. Table 1 summarizes the governing equations for a group of fractional order models. Fig. 12 shows, for a fixed set of model parameters, the order for which each system exhibits chaotic behavior. For the models examined, the Lorenz system showed the narrowest range for chaos ($0.9941<q<1$), whereas the NSG system showed the widest range ($0.7521<q<1$).

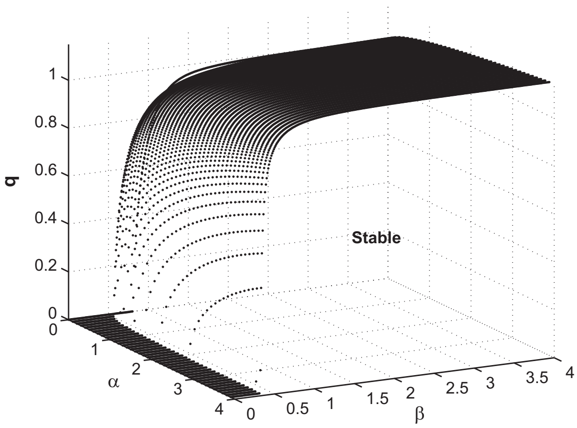

Fig. 11. Comparison of the stability region for the fractional order NSG system versus α and β for $k=10.5$.

Table 1
Selected examples of chaotic systems ($0.9941<q<1$).

System	Dynamics
Lorenz	$\begin{cases} D^q x = 10(y-x) \\ D^q y = x(28-z)-y \\ D^q z = xy-\frac{8}{3}z \end{cases}$
Chen	$\begin{cases} D^q x = 35(y-x) \\ D^q y = 25x-xz+28y \\ D^q z = xy-3z \end{cases}$
Lü	$\begin{cases} D^q x = 36(y-x) \\ D^q y = -xz+20y \\ D^q z = xy-3z \end{cases}$
Liu	$\begin{cases} D^q x = -x-y^2 \\ D^q y = -4xz+2.5y \\ D^q z = 4xy-5z \end{cases}$
Rössler	$\begin{cases} D^q x = -y-z \\ D^q y = x+0.2y \\ D^q z = 0.2+z(x-5.7) \end{cases}$
Newton-Leipnik	$\begin{cases} D^q x = 0.4x+y+10yz \\ D^q y = -x-0.4y+5xz \\ D^q z = 0.175z-5xy \end{cases}$
Financial	$\begin{cases} D^q x = z+(y-1)x \\ D^q y = 1-0.1y-x^2 \\ D^q z = -x-z \end{cases}$
Volta	$\begin{cases} D^q x = -x-19y-zy \\ D^q y = -y-11x-xz \\ D^q z = 0.73z+xy+1 \end{cases}$
FNSG	$\begin{cases} D^q x = -0.75x+y \\ D^q y = -x-0.75y(1-10.5z) \\ D^q z = 0.75(0.15(1-z)-ky^2) \end{cases}$
RD	$\begin{cases} D^q x = -0.4\pi y+30z(0.1721x-0.9851y)-0.4x \\ D^q y = 0.4\pi x-z+30z(0.1721y+0.9851x)-0.4y \\ D^q z = y-5.1642(x^2+y^2)-0.2(z-1) \end{cases}$

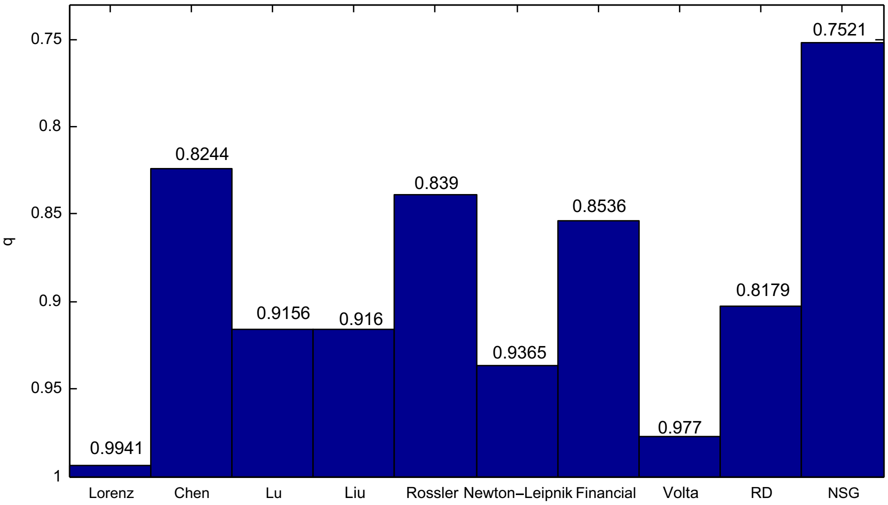

Fig. 12. Comparison of the chaotic regions of classic chaotic systems.

Moving down Table 1 from the Lorenz to the RD case, the models, in general, become more nonlinear. We note, for example, that the Rössler chaotic system has just one nonlinearity (xz in the third equation), while in the Lorenz, Chen, and Lü systems the nonlinearities occur both in the second equation (xz) and in the third equation (xy). A new nonlinearity term (y^2) appears in the first equation of Liu systems, and Newton–Leipnik systems have nonlinear terms in all three equations, which makes their dynamics more complicated. The Financial system, the Rössler and the Volta models are examples of systems with a constant added in one of the equations, which results in a system without the zero equilibrium points. The Volta system and the Newton–Leipnik systems have the same core nonlinear terms, but they exhibit different chaotic behavior. The FNSG system is very similar to the classic models shown above, with only two nonlinear terms, plus a constant, thus it is somewhat surprising that it exhibits the full spectrum of chaotic behavior. The radiation damping model (RD) is quite a bit more complex when compared with the other well-known chaotic systems. This is largely due to its derivation from fundamental NMR phenomena, Hamri and Houmor [11], where internal feedback generates the xz and xy cross terms in the first two equations, and the squared terms x^2 and y^2 in the third equation; nevertheless, the chaotic behavior in the fractional order system is considerable. In fact, a simple generalization of the Sherman experiment, [5], using pairs of RF coils on both the x and the y axes, gives the same cross terms. So, all together, the FNSG system provides a good case study for chaos and a simple model of the effects of feedback in NMR.

Finally, it should be noted that the chaotic behavior in the selected systems should be studied in both the transient and Steady state responses. However, transient chaos is not a critical concern in control applications of chaos. Therefore, in this paper we studied the occurrence of steady-state chaos in the FNSG system using a bifurcation diagram. But, in order to provide a fair comparison with other systems, the transient response of the FNSG was also included in the results shown in Table 1. More explicitly, the FNSG system studied in Table 1 shows chaotic behavior including transient chaos only for $q > 0.7521$, but when considering just the steady-state response, this system shows chaotic behavior for $0.751 < q < 0.795$ and $0.978 < q < 1$ (see bifurcation diagram shown in Fig. 8(a)).

5. Conclusion

Chaos in the fractional order spin generator system is studied in this paper. The FNSG has been shown by both theoretical and numerical methods to exhibit chaotic behavior for the fractional derivative order $q \geq 0.7521$ for the selected damping parameters. This behavior extends over a relatively larger range than several of the commonly studied fractional order systems. In addition, the nonlinear characteristics of the FNSG system provide a good case study for the onset of chaos in a fractional order system. The application of FNSG in NMR demonstrates its potential as a model system for demonstrating chaotic behavior in the laboratory, and the extension of this model to clinical imaging systems may provide a domain for future control applications in MRI.

Acknowledgments

The authors would like to thank the reviewers for their helpful comments and Ms. Oviya Thanigaivelan for her assistance in the preparation of the paper.

References

[1] M. Kac, Some mathematical models in science, Science 166 (1969) 695–699.
[2] A. Abragam, Principles of Nuclear Magnetism, Oxford University Press, USA, 2002.
[3] P. Callaghan, Principles of Nuclear Magnetic Resonance Microscopy, Clarendon Press, Oxford, 2004.
[4] E. Haacke, R. Brown, M. Thompson, R. Venkatesan, Magnetic Resonance Imaging: Physical Principles and Sequence Design, vol. 82, Wiley-Liss, New York, 1999.

[5] S. Sherman, A third-order nonlinear system arising from a nuclear spin generator, Contrib. Differ. Equat. 2 (1963) 197.
[6] P. Sachdev, R. Sarathy, Periodic and chaotic solutions for a nonlinear system arising from a nuclear spin generator, Chaos Solitons Fractals 4 (11) (1994) 2015–2041.
[7] D. Abergel, Chaotic solutions of the feedback driven Bloch equations, Phys. Lett. A 302 (1) (2002) 17–22.
[8] J. Park, Chaos synchronization of nonlinear Bloch equations, Chaos Solitons Fractals 27 (2) (2006) 357–361.
[9] Q. Yuan, X. Yang, Computer-assisted verification of chaos in the model of nuclear spin generator, Appl. Math. Comput. 213 (1) (2009) 148–152.
[10] C. Ahn, Chaos synchronization of nonlinear Bloch equations based on input-to-state stable control, Commun. Theoret. Phys. 53 (2) (2010) 308.
[11] N. Hamri, T. Houmor, Chaotic dynamics of the fractional order nonlinear Bloch system, Electron. J. Theoret. Phys. 8 (25) (2011) 233–244.
[12] J. Jeener, Dynamical effects of the dipolar field inhomogeneities in high-resolution nmr: spectral clustering and instabilities, Phys. Rev. Lett. 82 (8) (1999) 1772–1775.
[13] S. Huang, J. Walls, Y. Wang, W. Warren, Y. Lin, Signal irreproducibility in high-field solution magnetic resonance experiments caused by spin turbulence, J. Chem. Phys. 121 (13) (2004) 6105–6109.
[14] D. Abergel, A. Louis-Joseph, Generating spin turbulence through nonlinear excitation in liquid-state nmr, J. Mag. Reson. 196 (2) (2009) 115–118.
[15] J. Schiano, R. Magin, S. Wright, Feedback control of the nuclear magnetization state: modeling and control design, IEEE Trans. Med. Imag. 10 (2) (1991) 138–147.
[16] J. Schiano, A. Webb, R. Magin, Feedback control of the nuclear magnetization state: experimental results, IEEE Trans. Med. Imag. 11 (2) (1992) 203–214.
[17] D. Ghosh, A. Chowdhury, P. Saha, Bifurcation continuation, chaos and chaos control in nonlinear Bloch system, Commun. Nonlinear Sci. Numer. Simul. 13 (8) (2008) 1461–1471.
[18] A. Uçar, K. Lonngren, E. Bai, Synchronization of chaotic behavior in nonlinear Bloch equations, Phys. Lett. A 314 (1) (2003) 96–101.
[19] F. Kakmeni, J. Nguenang, T. Kofané, Chaos synchronization in bi-axial magnets modeled by Bloch equation, Chaos Solitons Fractals 30 (3) (2006) 690–699.
[20] R. Magin, X. Feng, D. Baleanu, Solving the fractional order Bloch equation, Concept. Mag. Reson. Part A 34 (1) (2009) 16–23.
[21] I. Petráš, Modeling and numerical analysis of fractional-order Bloch equations, Comput. Math. Appl. 61 (2) (2011) 341–356.
[22] S. Bhalekar, V. Daftardar-Gejji, D. Baleanu, R. Magin, Generalized fractional order Bloch equation with extended delay, Int. J. Bifurc. Chaos 22 (04) (2012) 125071–125086.
[23] I. Podlubny, Fractional Differential Equations. An Introduction to Fractional Derivatives, Fractional Differential Equations, Some Methods of Their Solution and Some of Their Applications, Academic Press, San Diego, New York, London, 1999.
[24] K. Diethelm, N. Ford, A. Freed, A predictor–corrector approach for the numerical solution of fractional differential equations, Nonlinear Dyn. 29 (1) (2002) 3–22.
[25] K. Diethelm, An algorithm for the numerical solution of differential of fractional order, Electron. Trans. Numer. Anal. 5 (1) (1997) 1–6.
[26] K. Diethelm, N. Ford, Analysis of fractional differential equations, J. Math. Anal. Appl. 265 (2) (2002) 229–248.
[27] R. Garrappa, 2012, URL ⟨http://www.dm.uniba.it/nagb/?q=node/17⟩.
[28] K. Diethelm, N. Ford, A. Freed, Detailed error analysis for a fractional Adams method, Numer. Algorithms 36 (1) (2004) 31–52.
[29] M. Tavazoei, M. Haeri, Chaotic attractors in incommensurate fractional order systems, Phys. D: Nonlinear Phenom. 237 (20) (2008) 2628–2637.
[30] L. Chua, M. Komuro, T. Matsumoto, The double scroll family, IEEE Trans. Circuits Syst. 33 (11) (1986) 1072–1118.
[31] J. Lu, G. Chen, X. Yu, H. Leung, Design and analysis of multiscroll chaotic attractors from saturated function series, IEEE Trans. Circuits Syst. I 51 (12) (2004) 2476–2490.
[32] W. Deng, J. Lü, Design of multidirectional multiscroll chaotic attractors based on fractional differential systems via switching control, Chaos: Interdiscip. J. Nonlinear Sci. 16 (4) (2006) 043120.
[33] W. Deng, J. Lü, Generating multi-directional multi-scroll chaotic attractors via a fractional differential hysteresis system, Phys. Lett. A 369 (5–6) (2007) 438–443.
[34] D. Matignon, Stability results for fractional differential equations with applications to control processing, in: Proceedings of the Computational Engineering in Systems Applications, 1996, pp. 963–968.
[35] I. Petráš, D. Bednárová, Fractional-order chaotic systems, in: Proceedings of the 14th IEEE International Conference on Emerging Technologies & Factory Automation, 2009, pp. 1031–1038.
[36] I. Petráš, Fractional-Order Nonlinear Systems: Modeling, Analysis and Simulation, Springer Berlin Heidelberg, 2011.
[37] S. Bhalekar, V. Daftardar-Gejji, D. Baleanu, R. Magin, Transient chaos in fractional Bloch equations, Comput. Math. Appl. 64 (2012) 3367–3376.